CS36-

Computers & Structures Vol. 36, No. 4, pp. 681–689, 1990
Printed in Great Britain.

0045-7949/90 $3.00 + 0.00
Pergamon Press plc

THREE-DIMENSIONAL DYNAMIC FINITE ELEMENT ANALYSIS FOR SHOT-PEENING MECHANICS

Y. F. AL-OBAID
Faculty of Technological Studies, PAAET, P.O. Box 42325, 70654 Shuwaikh, Kuwait

(*Received* 25 *July* 1989)

Abstract—A step-by-step dynamic finite element analysis is presented in which a provision is made for a three-dimensional isoparametric element existing in the target metal plate. On the basis of this analysis, the computer program OBAID has been modified for dynamic loading due to impinging shot. The target material is considered to be elastoplastic and the analysis allows for strain and work hardening. The problem is envisaged to embrace a process of multiple indentations which cover the surface of the target progressively, thus allowing for shakedown of each spot due to repeated impact and also saturation due to complete surface coverage.

INTRODUCTION

Shot-peening is a cold-working method that involves pelting the surface of a metal part with round metallic or glass shot thrown at a relatively high velocity ($\simeq 100$ m/sec).

Each shot acts as a tiny peen-hammer, making a small dent in the surface of the metal and stretching the surface rapidly as it hits. The impact of the shot causes plastic deformation which results in changes in the mechanical properties of the surface material. In other words, shot-peening can produce a substantial increase in surface hardness of a component as well as produce favourable residual stresses to increase fatigue life considerably. The general form of residual stress in a typical shot-peening operation is shown in Fig. 1.

The variety of items that are shot-peened is impressive; gears of all types and sizes, shafts with circlip grooves, bearing surfaces with section changes, steam and gas turbine parts, aircraft undercarriage parts, helicopter propeller drives and blades, compressor and high performance engine parts—pistons, crank shafts, connecting rods, valves and blocks. Probably the most exotic application of shot-peening is peen-forming. If you shot-peen one side of a sheet of metal the stretching of the peened surface causes the sheet to develop a spherical curvature, convex on the peened side. By exercising rigid controls in this process, the panels that cover the wings of most of the larger aircraft can be peened to exact aerodynamic profiles.

There are many parameters involved in shot-peening which must be accurately controlled and regulated in order to produce a compressively stressed surface layer in which the amount of stress, the uniformity of the stress, and the depth of the layer can be held constant from piece to piece. These parameters are the type and size of shot, angle of impact, time of exposure and the extent of surface coverage.

Although the process of shot-peening is well developed and is in successful daily use, the science is just beginning to be understood and the theory still represents a controversial field. This is due to the complexity of the process, which still requires further study and research. This paper attempts to present a theoretical model using a three-dimensional isoparametric finite element; as will be seen, it surprisingly agrees reasonably well with other models [1–3].

THREE-DIMENSIONAL FINITE ELEMENT MESH GENERATION

The finite element mesh for the target plate is shown in Fig. 2. In order to produce accurate residual stresses, it has been decided to divide the thickness of the target steel plate into nine layers (in the Y-direction). The plate thickness below the neutral axis is divided into two equal layers each of 0.0079 m. Immediately above the neutral axis, the thickness of the first layer is 0.00397 m. Above this layer there are six equal layers each of 0.00198 m thickness. A flexibility exists for various plane meshes of variable dimensions. A quarter of the actual size of the target plate is chosen for the shot-peening analysis based on the finite element technique. Hence a mesh contains 81 elements of the 20-noded isoparametric shapes, as shown in Fig. 3. The numbering scheme adopting is based on a right hand rule. Each element is numbered together with eight specific Gauss points ($2 \times 2 \times 2$) in the manner shown in Fig. 4. The position of each Gauss point within each element is indicated in Fig. 5.

IMPACT LOAD CRITERIA

An attempt has been made to study the mechanics of a single shot indentation due to both static and dynamic loading using the theoretical model and the computer program OBAID [4]. The shot is assumed

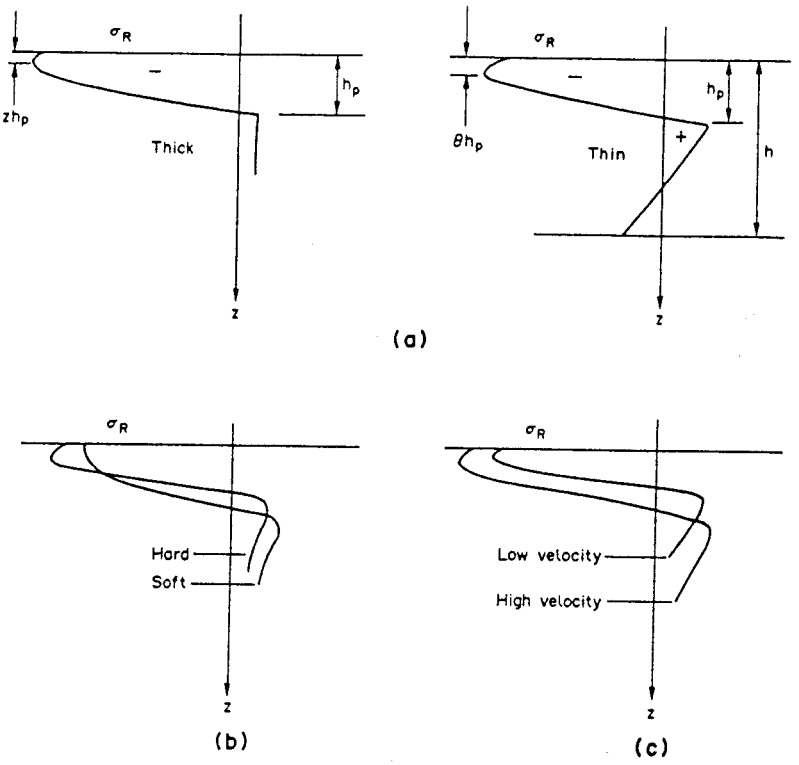

Fig. 1. Typical residual stress distribution in shot-peening operation.

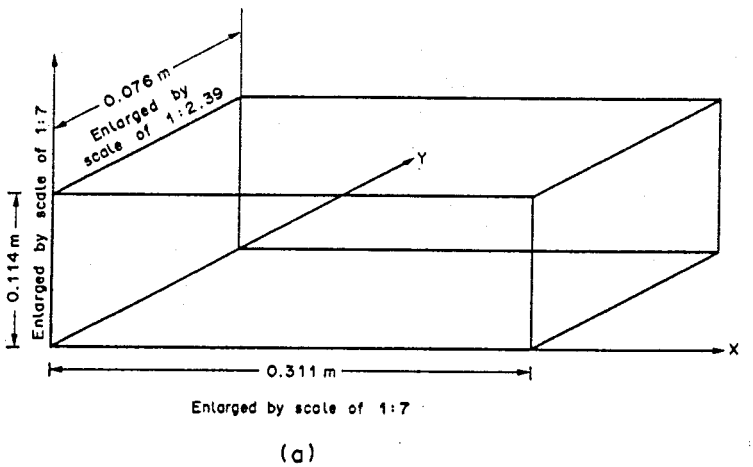

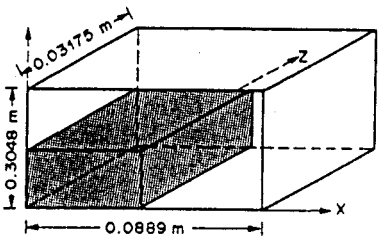

Fig. 2. Plate size. (a) Enlarged by scale 1 : 7. Note: the dimensions of the mesh have not been enlarged proportionally; the size of the mesh provided is enlarged to the sizes shown. (b) Shaded area is a quarter of the target plate.

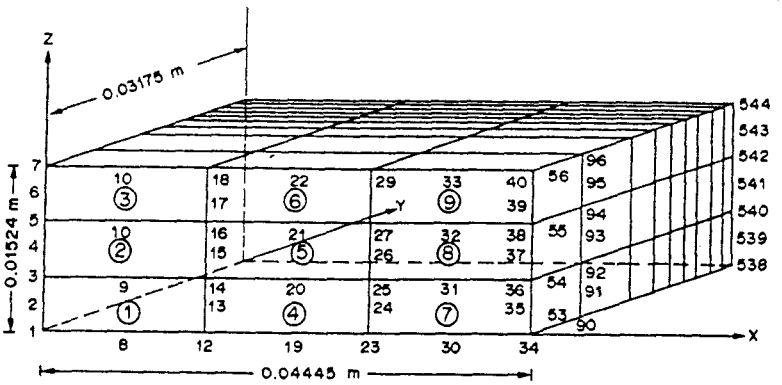

Fig. 3. True dimensions of mesh containing 81 elements; elements are numbered as shown.

rigid and undeformable while the target material receives indentations. Low and high velocity ranges have been considered together with the contact time. The shot velocity ranges come from the data available from a series of tests carried out by the author. These have been simulated in order to process specific results.

It is essential to enlarge upon the basic criterion. The rigid steel shot is assumed to strike, with a gradually increasing load, on the steel target plate. This increasing load is imposed on each surface element, one at a time. The patch load in effect acts, during loading and unloading, on each surface element, exciting all the other elements through the connectivity model which links all the elements together. The second loading is then applied on the adjacent surface element, but this time all the residual displacements and residual stresses from the previous impact are allowed for. Therefore, the response of the target will be different. By storing and updating the state of the target the cumulative result is then plotted in a three-dimensional space. The process is repeated until the whole surface is covered more than once, so that each spot is loaded several times, the number of times depending upon the duration of the process.

STEP-BY-STEP FINITE ELEMENT ANALYSIS

Apply a load increment, $\{\Delta F_n\}$, where n is the load increment.

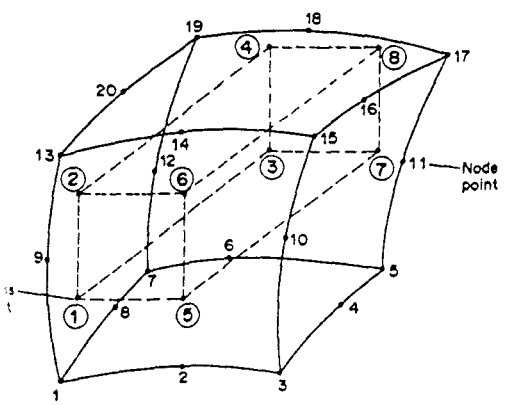

Fig. 4. Element numbering and Gauss points.

2. Accumulate total load $\{F_n\} = \{F_{n-1}\} + \{\Delta F_n\}$ and $\{R\} = \{F_n\}$, where $\{R\}$ is the residual load vector.
3. Solve $\{\Delta u_i\} = [K]^{-1}\{R\}$, where i is the iteration.
4. Accumulate total displacements

$$\{U_i\} = \{U_{i-1}\} + \{\Delta U_i\}.$$

5. Calculate strain increments as

$$\{\Delta\epsilon_i\} = [B]\{\Delta U_i\}$$

and strains as

$$\{\epsilon_i\} = \{\epsilon_{i-1}\} + \{\Delta\epsilon_i\}.$$

6. The stress increments are calculated using the current non-linear constitutive matrices. For steel target plate elastoplastic relations are expressed in the general form

$$\{\Delta\sigma_i\} = \{f(\sigma)\}\{\Delta\sigma\}.$$

Accumulate stresses as

$$\{\sigma_i\} = \{\sigma_{i-1}\} + \{\Delta\sigma_i\}.$$

ISP = stress point
= 0—elastic point
= 1—plastic point
= 2—unloading from plastic state
σ_y = uniaxial yield stress.

6.1. Firstly, the stress increment is calculated using the elastic material matrix as $\{\Delta\sigma_i\} = [D]^e_e\{\Delta\epsilon\}$, where $[D]^e_e$ is the elastic material matrix for steel target plate. First estimate of total stress:

$$\{\sigma'_i\} = \{\sigma_{i-1}\} + \{\Delta\sigma'_i\}.$$

6.2. Calculate

$$\{\bar{\sigma}_i\} = \{f(\sigma'_i)\}$$

$$\{\bar{\sigma}_{i-1}\} = \{f(\sigma_{i-1})\}$$

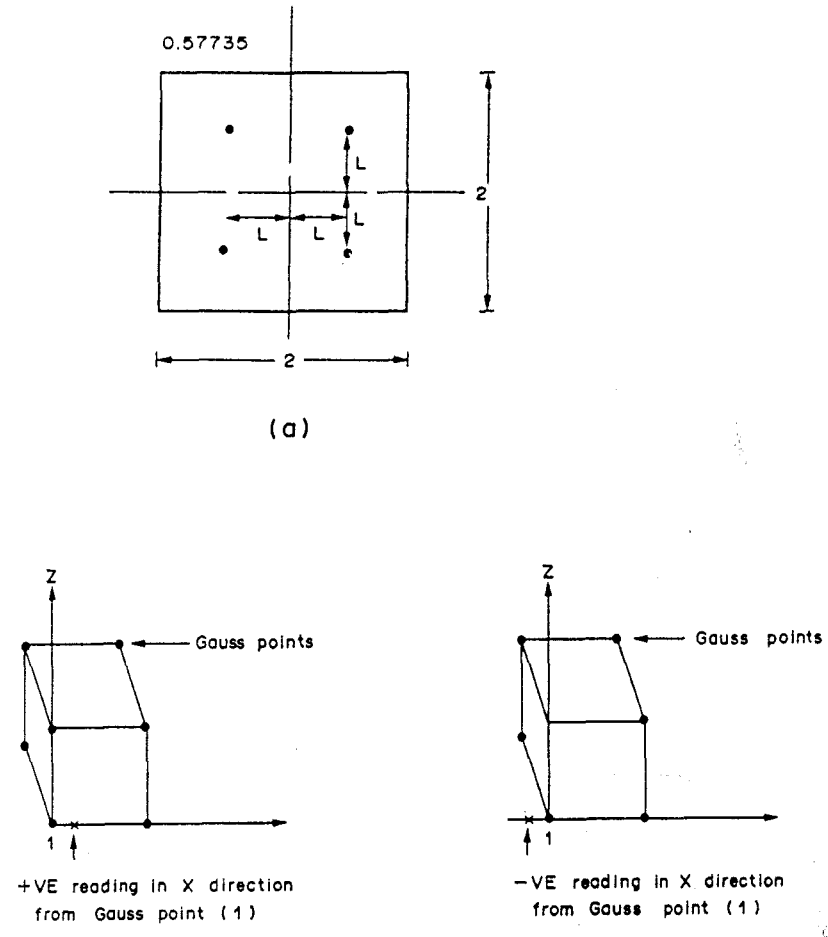

Fig. 5. Positioning of Gauss points within the element.

using von Mises yield criterion or another yield criterion.

6.3. If plastic point (i.e. $ISP = 1$), go to step 6.5.

6.4. If $\bar{\sigma} \geqslant \sigma_y$—plastic point ($ISP = 1$), transition from elastic to plastic, calculate factor f_{TR}.

$$f_{TR} = \frac{\sigma_y - \sigma_{i-1}}{\bar{\sigma} - \sigma_{i-1}}.$$

Stress at yield surface

$$\{\sigma_i\}^y = \{\sigma_{i-1}\} + f_{TR} \times \{\Delta\sigma_i\}.$$

Calculate elasto-plastic stress increment

$$\{\Delta\sigma_i\} = [D]^y_{ep}\{\sigma_i\}^y \times (1 - f_{TR})\{\Delta\epsilon\}.$$

Total stress

$$\{\sigma_i\} = \{\sigma_i\}^y + \{\Delta\sigma_i\}.$$

Set $ISP = 1$; go to 6.7.

If $\bar{\sigma}_i < \sigma_y$—elastic point, $\sigma_i = \sigma'_i$; go to step 6.8.

6.5. Plastic point in the previous iteration, check for unloading, i.e. $\sigma \geqslant \sigma_y$ (set Fig. 6); go to step 6.6. Unloading at this point, set $ISP = 2$, total stress.

$$\{\sigma_i\} = \{\sigma_{i-1}\} + \{\Delta\sigma_i\}$$

and set

$$\{\sigma_y\} = \{\bar{\sigma}_{i-1}\};$$

go to step 6.8.

6.6. Loading at this point

$$\{\Delta\sigma_i\} = [D]^y_{ep}\{\sigma_{i-1}\}\{\Delta\epsilon\}.$$

Total stress

$$\{\sigma_i\}_T = \{\sigma_{i-1}\} + \{\Delta\sigma_i\}.$$

Let $[D']$ be the stiffness matrix of an element in the global direction at the beginning of the

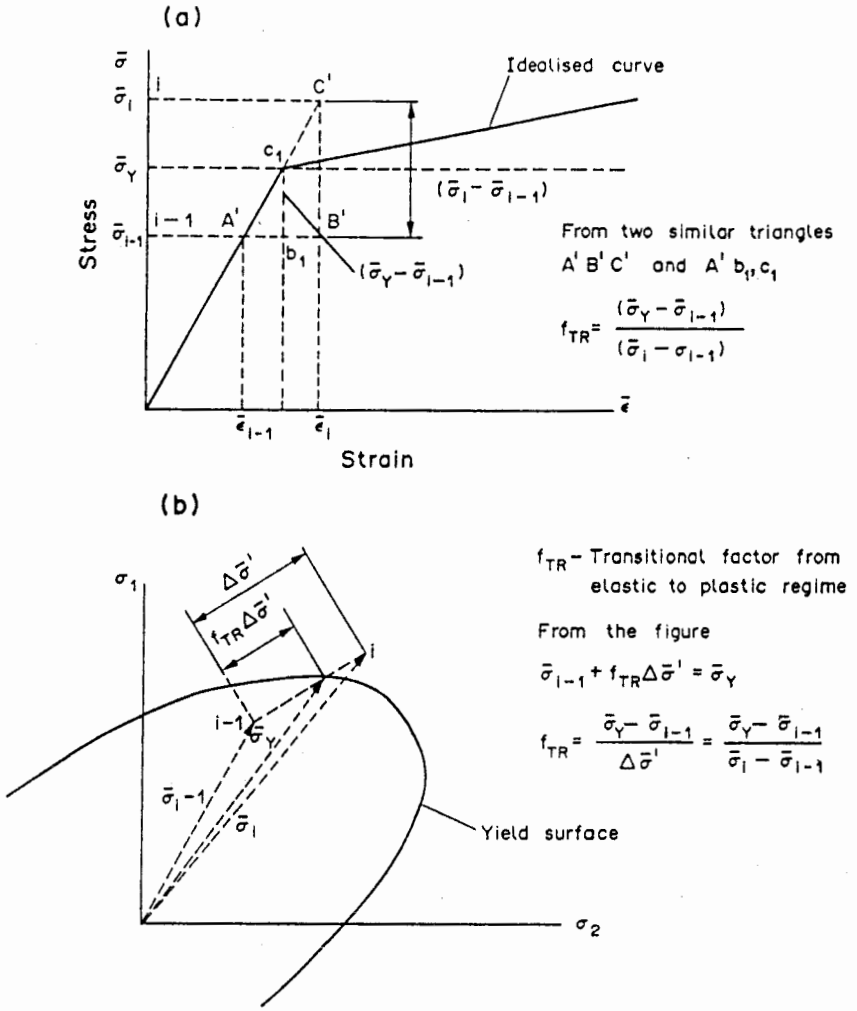

Fig. 6. (a) Equivalent stress–strain curve for steel plate. (b) Yield surface in the principal stress axes.

increment of the nth iteration within the increment; then

$$\{\Delta\sigma_n\}_{x,y,z} = [D]_x\{\Delta\epsilon_n\}_{x,y,z},$$

where $\{\Delta\sigma_n\}_x$ and $\{\Delta\epsilon_n\}_x$ are the resulting stresses and strains of the element in this iteration. The total stresses at the end of the iteration in this element are given by

$$\{\Delta\sigma_n\}^u_{x,y,z} = \{\sigma_{n-1}\}_{x,y,z} + \{\Delta\sigma_n\}_{x,y,z},$$

where $\{\sigma_{n-1}\}_{x,y,z}$ is the total balanced stress at the previous $(n-1)$th iteration. Let the principal stresses corresponding to global total stress be $\{\sigma_n\}^u_p$, i.e.

$$\{\sigma_n\}^u_p = [T_\epsilon^{-1}]^T\{\sigma_n\}_{x,y,z},$$

where

$$[T_\epsilon] = \begin{bmatrix} c^2 & s^2 & sc \\ s^2 & c^2 & -sc \\ -2sc & 2sc & c^2-s^2 \end{bmatrix}$$

$$[T_\epsilon]^{-1} = \begin{bmatrix} c^2 & s^2 & -sc \\ s^2 & c^2 & sc \\ -2sc & -2sc & c^2-s^2 \end{bmatrix};$$

s = sine and c = cosine.

From the constitutive relations in the principal direction the stresses are given by

$$\{\sigma_n\}_p = [\{\epsilon_n\}].$$

The unbalanced stresses in the principal direction are given by

$$\{\Delta\sigma_n\}_p = \{\sigma_n\}^u_p - \{\sigma_n\}_p$$

and unbalanced stresses in global direction (x) are found as

$$\{\Delta\sigma\}^u_x = [T_\epsilon]^T\{\Delta\sigma_n\}^u_p.$$

These unbalanced stresses in the global direction are treated as initial stresses and are subtracted

from the total stresses $\{\sigma_n\}_x^u$ to obtain balanced stresses as

$$\{\sigma_n\}_x = \{\sigma_n\}_x^u - \{\Delta\sigma_n\}_x^u.$$

To maintain equilibrium, the equivalent balanced nodal forces are calculated as

$$\{F_n\}_x^u = \int_V [B]^T \{\Delta\sigma_n\}_x^u \, \mathrm{d\,vol},$$

and these forces are applied to the material surrounding the target. Having determined the incremental initial stresses at the integration points, the computation of incremental initial loads, and the iterative procedure of the resulting set of equations, is carried out in the manner explained above. To evaluate stresses and strains at the Gaussian integration points throughout the whole target an eight-point integration point mesh for isoparametric solid elements is adopted.

6.7. Stresses calculated using the elastoplastic material matrix do not drift from the yield surface, as shown in Fig. 6. The following correction is taken into consideration, based on the equivalent stress–strain curve:

$$\bar{\sigma}_{\mathrm{corr}} = \bar{\sigma}_{i-1} + H\,\Delta\bar{\epsilon}_p,$$

where

$$\Delta\bar{\epsilon}_p = \sqrt{(\tfrac{2}{3}\Delta\epsilon_{ij}^p\,\Delta\epsilon_{ij}^p)} = \tfrac{2}{3}a^T a\lambda$$

= equivalent plastic strain increment.

H is the strain hardening parameter, such that $\Delta\bar{\epsilon}_p = \lambda$. Equivalent stress is calculated from the current stress state

$$\{\bar{\sigma}_i\} = f\{(\sigma_i)\}$$

$$\text{factor} = \frac{\sigma_{\mathrm{corr}}}{\sigma}.$$

Therefore the correct stress on the yield surface is

$$\{\sigma_i\} = \text{factor} \times \{\sigma_i\}.$$

6.8. End.

7. The total stresses are converted into equivalent internal loads from

$$\int_V [B]^T \{\sigma_i\} \, \mathrm{d\,vol}$$

and the residual load vector is calculated from

$$\{R\} = \{F_n\} - \int_V [B]^T \{\sigma_i\} \, \mathrm{d\,vol}.$$

8. Check for convergence. Two types of convergence criteria are used. They are the residual and the displacement convergence. The Euclidean norms are tested as

$$(\|R\|/F_{\mathrm{ext}}\|) \leqslant \mathrm{TOL}$$

$$(\|\Delta U\|/\|U\|) \leqslant \mathrm{TOL},$$

where

$$\|R\| = \sqrt{(R_i^T R_i)}$$

is the Euclidean norm of the residuals;

$$\|F_{\mathrm{ext}}\| = \sqrt{(F_{\mathrm{ext}}^T F_{\mathrm{ext}})}$$

is the Euclidean norm of the externally applied load;

$$\|\Delta U\| = \sqrt{(\Delta U_i^T U_i^T)}$$

is the Euclidean norm of the incremental displacement;

$$\|U\| = \sqrt{(U_i^T U_i)}$$

is the Euclidean norm of the total displacements and the tolerance limit for impact is taken as 0.01.

If convergence is not achieved, go to step 3 and repeat all the steps for the next iteration. If the convergence is achieved, then go to step 1 and repeat the process with the next load increment.

THE PLOTTING OF RESULTS

At points of elastic unloading for normal residual stress, each Gauss point has three components: X, Y and Z. Some of these components are negative and some are positive. If this sign convention is adopted when plotting in the X-direction, for example, a positive sign would indicate a reading to the right of the Gauss point, and a negative sign would indicate the opposite direction, to the left of the Gauss point. Similarly, a positive sign in the Z-direction would indicate a reading above the Gauss point, and a negative sign would indicate a reading below the Gauss point. All points have been produced for the X–Y, X–Z and Y–Z planes (see Figs 3 and 7). The mesh contains 81 elements and 544 node points.

DISCUSSION ON THE ANALYSIS AND RESULTS

Throughout the analysis, the plastic strain increment is always assumed to be normal to the plastic potential. The plastic material matrix is determined so as to define the stress increment in the plastic region. Since it is necessary to satisfy the yield

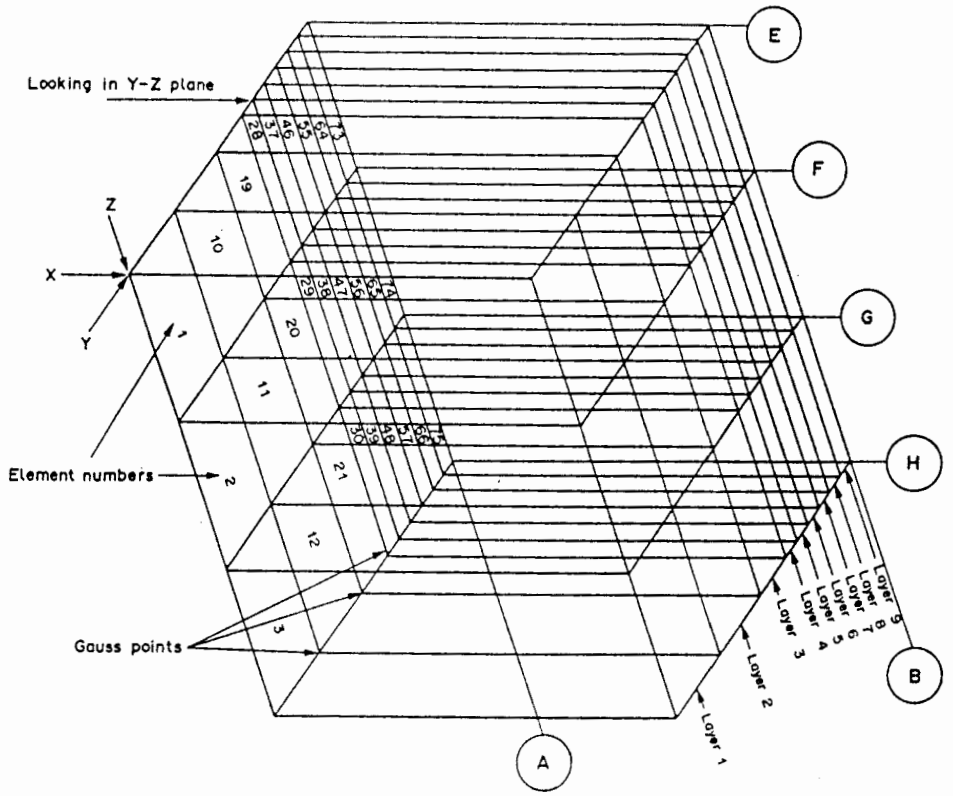

Fig. 7. Three-dimensional mesh for target plate.

unction, it is assumed that the stress must lie on he yield surface, such that the strain hardening unction depends on the plastic deformation. As ientioned earlier, at any stage of the impact oads produced by shots, these loads are auto-atically compared with the internal loads due total stress. The difference between the two loads is taken as a set of residual loads and the stresses caused can be interpreted as a measure of any lack of equilibrium. In order to maintain this equilibrium the residual loads applied and various parameters are computed. This process is repeated until the residual loads are sufficiently small for convergence [5, 6].

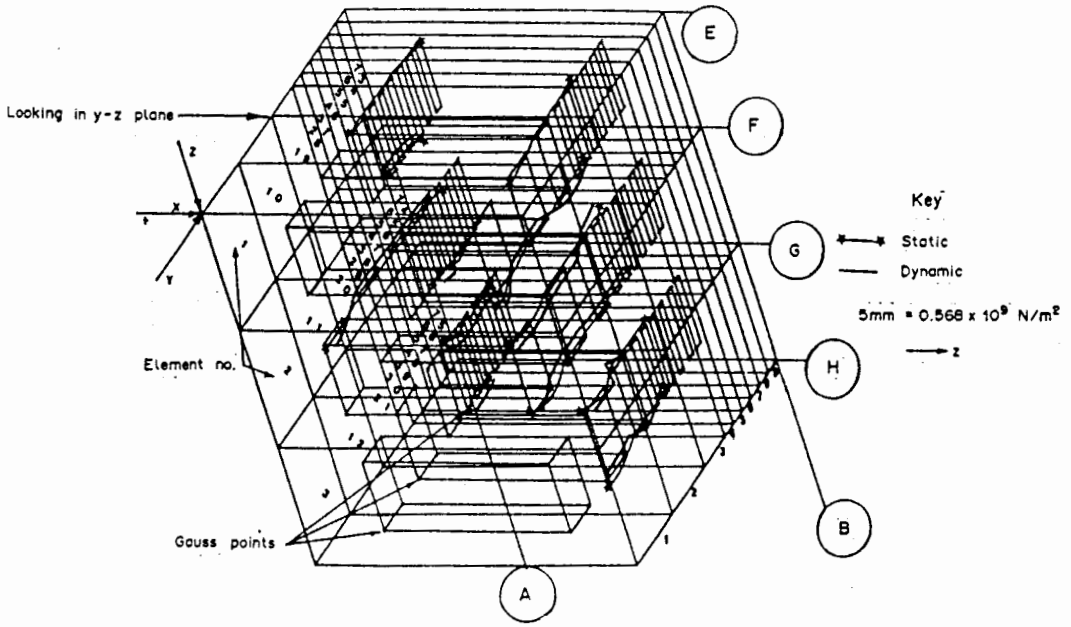

Fig. 8. Increment 2. Residual stresses. Section A–B.

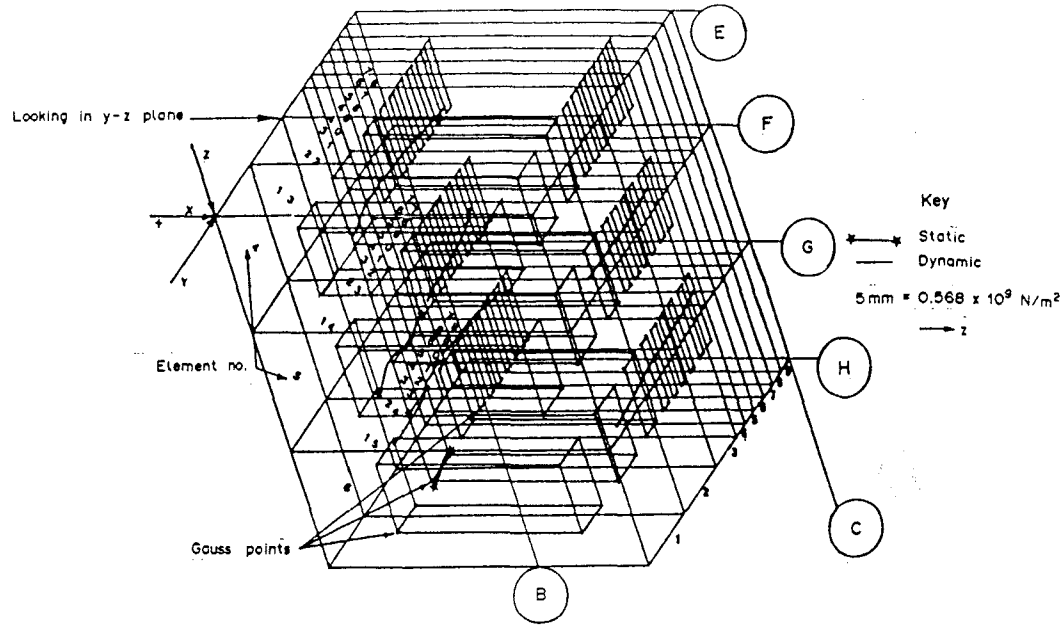

Fig. 9. Increment 2. Residual stresses. Section B–C.

All results have been plotted in three dimensions for three increments of loading from the output. The graphs plotted are the results of residual stresses; they show a three-dimensional mesh and three planes, namely the X–Y plane, the X–Z plane and Y–Z plane, are indicated on them. All graphs are along the thickness of the layers viewed in the Y–Z plane.

For the same mesh grading system under increment 2 both static and dynamic residual stresses viewed in the Y–Z plane are plotted (Figs 8 and 9). The magnitudes and positions of such stresses vary in both cases. Similarly, under increment 3 the residual stresses are plotted viewed first in the Y–Z plane (Figs 10 and 11). In the case of increment 3 much higher residual stresses are predicted. For comparison the residual stresses for the increment viewed in the X–Y plane are also drawn.

Such information is better visualized in the form of a distribution at the central plane through the thickness, as shown in Fig. 12. For comparison, the distribution as predicted from other models [1–3] is also shown.

It is concluded that the real plot of three-dimensional residual stresses can be plotted on the

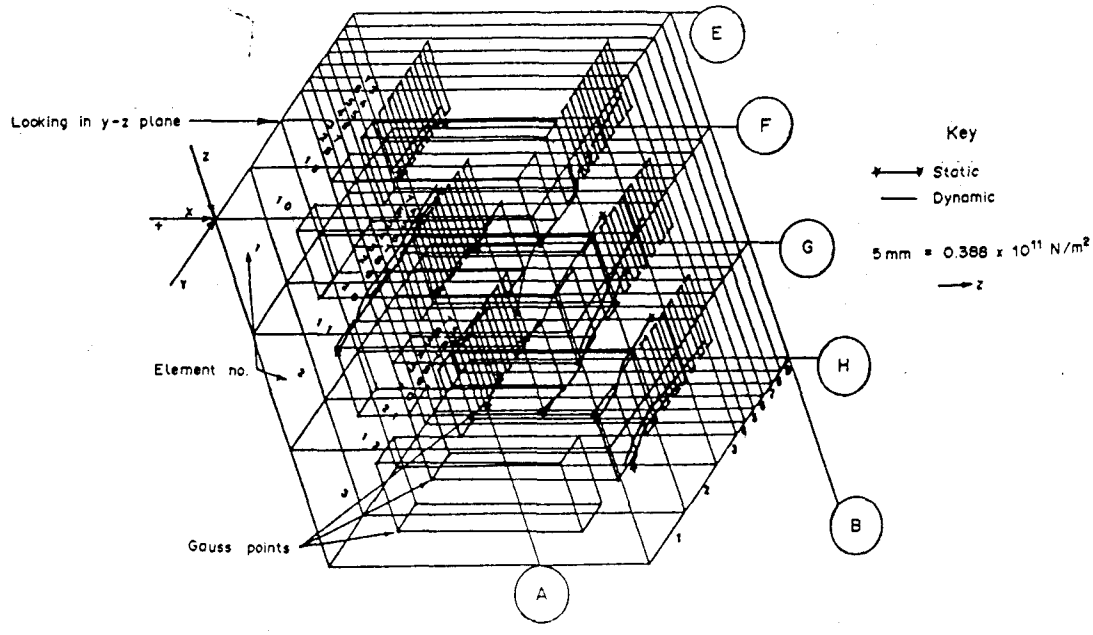

Fig. 10. Increment 3. Residual stresses. Section A–B.

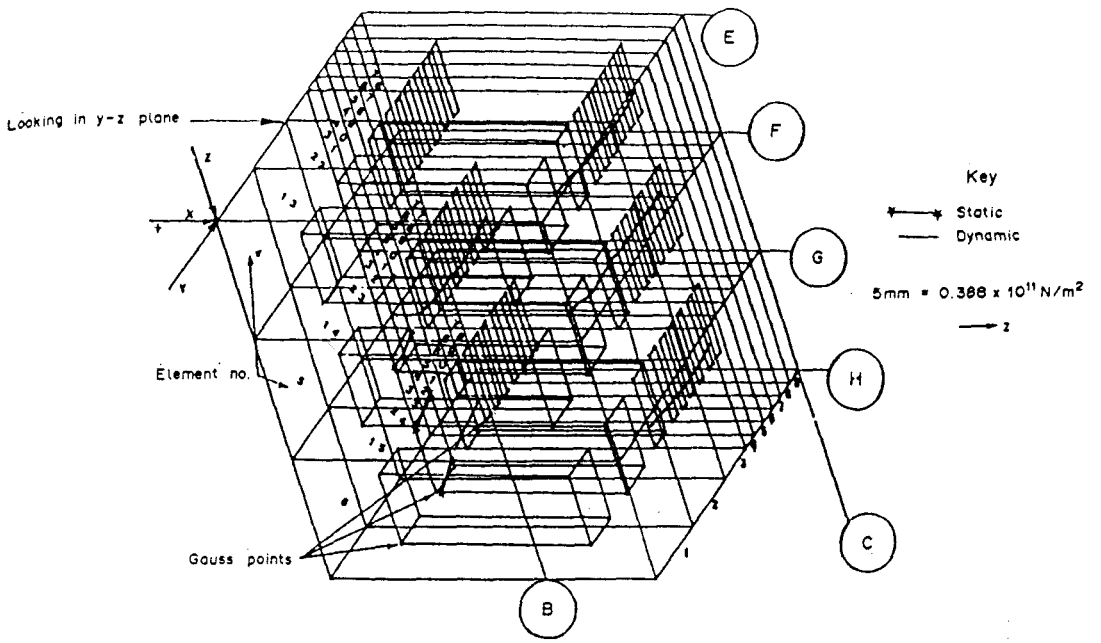

Fig. 11. Increment 3. Residual stresses. Section B–C.

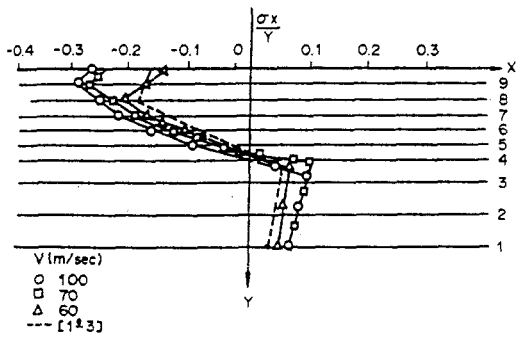

ig. 12. Residual stress distribution in X–Y central plane rough the thickness. Finite element, various velocities, shot size 0.7 mm diameter.

ree-dimensional mesh as when viewed in specific anes they would, in general, form a distribution rve of a cosine function.

CONCLUSIONS

A three-dimensional dynamic finite element analy- has been carried out to take into consideration stoplasticity. The solution procedures include an plicit version of direct integration with uniform acceleration and quick convergence associated with the initial stress approach. The steel target plate has been discretised into a series of solid isoparametric elements having nine layers within the plate thickness. The residual stress distributions obtained from finite element analysis are in a good agreement with those obtained by others [1–3].

REFERENCES

1. Y. F. Al-Obaid, Finite element approach to shot-peening mechanics. Proc. International Conference on Steel Structure, Yugoslavia, November 1986.
2. Y. F. Al-Obaid, A rudimentary analysis of improving fatigue life of metals by shot-peening. *J. appl. Mech., ASME* (accepted for publication).
3. S. T. S. Al-Hassani, Mechanical aspects of residual stress development in shot-peening. In *Proc. First International Conference on Shot-peening*. Pergamon Press, Oxford (1981).
4. Y. F. Al-Obaid, Numerical analysis of the laterally loaded piles in the Kuwait off-shore environment. *Int. J. Ocean Engng* **13**, 85–92 (1986).
5. K. J. Bathe and E. L. Wilson, Stability and accuracy analysis of direct integration method. *Int. J. Earthquake Enging struct. Dynam.* **1**, 289–291 (1977).
6. Y. Bangash, The structural integrity of concrete containment vessels under external impacts. 6th SMIRT Conference, Division J. No. 716, Paris, August 1981.